

# The structure of the binary phenol–methanol cluster: A comparison of experiment and ab initio theory

J. Küpper, A. Westphal, M. Schmitt \*

*Institut für Physikalische Chemie und Elektrochemie I, Heinrich-Heine-Universität Düsseldorf, Universitätsstrasse 26.43.02,  
D-40225 Düsseldorf, Germany*

Received 14 July 2000; in final form 11 October 2000

## Abstract

The structure, energetics, vibrations and barrier to internal rotation of the binary phenol–methanol cluster are calculated at different levels of theory and compared to the results of a rotationally resolved  $S_1 \leftarrow S_0$  electronic spectrum. The structure of the phenol–methanol cluster is determined by a hydrogen bond and by a dispersive interaction of the methyl group with the aromatic ring. To account for the correct balance between these two attractive forces, computational methods have been employed which include electron correlation. The barrier to internal rotation of the methyl group has been determined from the experiment and compared to the lowest energy path at a relaxed ab initio energy surface. Furthermore, an ab initio normal mode analysis is performed and compared to experimental intermolecular vibrational frequencies for both electronic states. © 2001 Elsevier Science B.V. All rights reserved.

## 1. Introduction

Hydrogen bonded clusters of phenol with water [1–13] and methanol [1,14–18] have been investigated in great detail both experimentally and theoretically, because they serve as model systems for larger aggregates. One of the priorities in these investigations is the experimental determination of the cluster structure and the comparison to calculated structures at different levels of theory.

An analysis of the structure of the phenol–water cluster in the  $S_0$  state with Fourier transform microwave spectroscopy [7] and in the  $S_0$  and  $S_1$  states using rotationally resolved LIF spectroscopy [6,19] yielded geometries, which compared

well to the calculated ab initio structure [5]. The relative orientation of the water moiety in the phenol–water cluster is mainly determined by the strength and the orientation of the hydrogen bond. Therefore ab initio calculations even on the HF level yield a geometry which nicely reproduces the one determined experimentally. In the case of phenol–methanol an additional interaction of the methyl group and the aromatic  $\pi$ -system may take place. The resulting structure represents a balance between both the dipole interaction, mainly responsible for the hydrogen bond and dispersive interactions, which describe the attractive forces between the methyl group and the  $\pi$ -system.

For the phenol–methanol cluster vibrational frequencies for the electronic ground state have been determined using dispersed fluorescence spectroscopy. The frequencies of two of these vibrations could be determined to be 22 and 162

\* Corresponding author. Tel.: +49-211-81-13681; fax: +49-211-81-15195.

E-mail address: mschmitt@uni-duesseldorf.de (M. Schmitt).

$\text{cm}^{-1}$ , respectively [14]. In the fluorescence excitation spectrum of the  $S_1$  state, Abe et al. [1] observed a vibronic band at  $27 \text{ cm}^{-1}$  which they assigned to a bending vibration and a band at  $175 \text{ cm}^{-1}$  which they assigned to the intermolecular stretching vibration.

To confirm that only one conformer of phenol( $\text{CH}_3\text{OH}$ )<sub>1</sub> is responsible for absorption in the observed spectral region, hole burning spectroscopy has been performed [17]. In this publication the six intermolecular vibrations both in the  $S_0$  and  $S_1$  state were assigned. Recently, a Fourier transform microwave spectrum of the phenol–methanol cluster has been taken by Gudladt in the group of Stahl [20], yielding rotational and centrifugal constants for the electronic ground state.

In a preceding publication we determined the structure of the phenol–methanol cluster by rotationally resolved UV spectroscopy [21]. Due to the torsional motion of the methyl group the vibronic origin is splitted into A and E subbands. From the analysis of the spectrum we could determine the position of the methanol moiety in the frame of the cluster. In conjunction the rotation-internal rotation coupling and the inertial parameters yielded a structure which will be compared in the following.

An analysis of the intermolecular vibrations in the electronic ground state has been published by Gerhards et al. [16]. Their calculations at the Hartree–Fock level predicted a translinear geometry, as in the case of the phenol–water cluster. Courty et al. [18] present a different structure of the cluster, based on a semi empirical model potential in which the methyl group of the methanol moiety is bent considerably towards the aromatic ring, which results in a hydrogen bond which is no longer linear.

Another possibility to determine the structures of the binary clusters is the comparison of calculated vibronic frequencies to experimental spectra. This gives an indirect check of the quality of the calculated structures. Nevertheless, cancellation of errors regarding the calculated force constants and structures reduce the reliability of such structures. We will show that in the case of the phenol–methanol cluster the evaluation of vibrational frequencies is not sufficient for a reliable determi-

nation of the structure, and may lead to wrong results.

In this work we give our main attention to the balance between hydrogen bonding of the hydroxy groups of phenol and methanol, respectively and the van der Waals interactions between the methyl group and the aromatic ring, which both determine the structure of the cluster. Furthermore the intermolecular vibrations and the barrier to internal rotation of the methyl group in the cluster are analyzed.

## 2. Computational methods

All ab initio calculations were performed using the GAUSSIAN 98 program package [22]. The SCF convergence criterion used for our calculations was an energy change below  $10^{-8}$  hartree, while the convergence criterion for the gradient optimization of the molecular geometry was  $\partial E/\partial r < 1.5 \times 10^{-5}$  hartree bohr<sup>-1</sup> and  $\partial E/\partial \varphi < 1.5 \times 10^{-5}$  hartree degree<sup>-1</sup>, respectively. The structure optimizations for the electronic ground state have been performed at the HF, MP2 and MP4(SDQ) level and with different density functional methods. While MP2 and MP4 account for dynamic electron correlation, the density functional methods only partially include correlation. We used the local spin density approximations (LSDA) [23,24], the BLYP functional [25,26], which does not contain Hartree–Fock exchange and the gradient corrected hybrid functional B3LYP [24–26], which includes partially HF exchange. The DFT as well as the MP2 calculations have been performed using Pople’s 6-31G(d,p), 6-311G(d,p) and 6-31++G(d,p) split valence basis sets as well as Dunning’s augmented correlation consistent basis set of double zeta quality (aug-cc-pVDZ).

Several starting geometries for the structure optimizations have been tried. A structure in which the methanol moiety is  $\pi$ -bound to the aromatic ring, and a second in which methanol acts as proton donor with respect to phenol have not converged at HF and MP2 level. For some of the optimized structures a normal mode analysis utilizing the analytical second derivatives of the potential energy surface has been performed in order

to obtain the intermolecular vibrational frequencies.

The geometry and the intermolecular vibrational frequencies of the first excited singlet state have been calculated with the CIS method using Pople's 6-31G(d,p) basis set. Because the description of clusters in the electronic ground state required the inclusion of dynamical electron correlation, reliable results for electronically excited states can only be expected using correlated methods for the  $S_1$  state like CASPT2. To describe the correlation interaction correctly six  $\pi$ -electrons of phenol, the oxygen lone pairs of phenol and methanol as well as the  $\sigma$ -electrons or the corresponding group orbitals of the methyl group have to be taken into account. To describe the effects under investigation this would require an active space that is too large to currently allow these calculations.

Approximate CPU times for a single point energy and frequency calculation, using the 6-31G(d,p) basis set on a SGI Origin 2000 machine are 2.5 h for HF, 4 h for CIS, 9 h for B3LYP and 23 h for MP2. CPU time for a single point energy calculation at MP4 level amounts to 26 h. No frequencies have been calculated at this level. The computational efforts for single point and frequency calculations with respect to different basis sets at MP2 level are 23 h for 6-31G(d,p), 91 h for 6-31G++(d,p) and 101 h for 6-311G(d,p).

In order to study the internal rotation of the methyl group we followed two different strategies. Both concern the question how to define a torsional coordinate in the cluster of methanol with phenol. A simple rotation about the torsional axis of methanol certainly is not adequate, due to interactions of the methyl group with the aromatic, which vary with the torsional angle. We therefore defined the torsional angle as dihedral angle which is formed by the plane H(methyl)–C–O with the plane C–O–H(hydroxyl) in the methanol moiety, letting all other intermolecular parameters including those of the methyl group relax. This procedure results in a complicated multidimensional motion, but has the advantage that the trajectory along this path represents a lower boundary for the value of the barrier connecting the two minima. A normal mode analysis for the geometry at the top of the

potential has been performed, in order to prove that it is a first order saddle point. The vibrational motion with negative frequency represents the torsional path. Xu et al. [27] have shown for the methanol monomer, that a very accurate barrier to internal rotation can be obtained at high level of theory and under inclusion of ZPE correction for the  $3n - 7$  "low amplitude" vibrations. This correction, however cannot be made for the phenol–methanol cluster, because due to the low frequency intermolecular vibrations, the separation into one large amplitude motion and "high frequency vibrations" cannot be performed. Thus the low frequency intermolecular vibrations mix to a considerable amount with the large amplitude motion, so that the vibrational mode which is equivalent to the passage over the saddle point cannot be identified uniquely. The so obtained transition state structure for the phenol–methanol cluster was compared to a transition state which was optimized by the synchronous transit-guided quasi-Newton method (STQN) [28,29], implemented in the GAUSSIAN 98 program package [22].

### 3. Results and discussion

#### 3.1. Geometries and energetic data

The experimental determination of the structural parameters of phenol(CH<sub>3</sub>OH)<sub>3</sub> from rotationally resolved UV spectroscopy has been described in detail elsewhere [21]. In the following, the experimental structure obtained from the high resolution experiment will be compared to calculated structures of the cluster, followed by an interpretation of the vibrational spectrum of phenol–methanol, which has been published before [17].

From the analysis of the rotationally resolved spectrum the rotational constants, as well as the direction cosines  $\lambda_g$  of the internal rotor axis with the inertial axes of the cluster were obtained. Due to the fact that the direction cosines are not linearly independent, only two of them can be determined independently. In order to describe the relative orientation of the two monomer units in a binary cluster six internal coordinates are needed.

The determination of three rotational constants and two direction cosines just allows for the calculation of five structural parameters. Thus one of the intermolecular parameters has to be kept fix. If we describe the methanol moiety as a dumbbell which connects the centers of mass of the hydroxyl and the methyl group, the rotational degree of freedom about this axis is lost.

Furthermore, the orientation of the internal rotor axis is not unambiguously defined because the signs of the direction cosines cannot be determined from the experiment. From the four distinguishable combinations of signs of two experimentally determined direction cosines and the indeterminable direction of the dumbbell, we expect eight different geometries.

Four of these in which the methyl group of the methanol moiety points towards the hydroxy group of phenol can be excluded by chemical reasoning. The structural parameters for the remaining four orientations of the methanol dumbbell are given in Table 2 for the ground state and in Table 4 for the electronically excited state. The orientation of this dumbbell in the electronic ground state of the cluster is shown in Fig. 1. Although the absolute signs could not be determined, a change of sign for a single  $\lambda_g$  upon electronic excitation can be excluded from the analysis of the transition intensities.

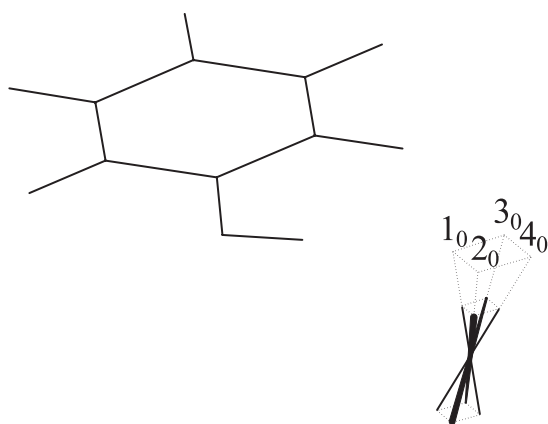


Fig. 1. The four possible orientations of the line connecting the center of mass of the methyl group and center of mass of the hydroxyl group, relative to the phenol molecule in the  $S_0$  state. The different ground state geometries are labeled  $1_0$ – $4_0$ .

Starting from this point one can deduce the structure of the cluster with only a few assumptions based on chemical reasoning or comparison to similar hydrogen bonded clusters. Due to the larger acidity of phenol relative to methanol it is most likely that phenol acts as proton donor as in the phenol–water and phenol–ammonia clusters. The proton accepting methanol is assumed to be oriented in a way that one of its oxygen lone pairs points towards the phenolic–OH group. Furthermore it has to be assumed that the geometry of the methanol moiety changes only slightly upon cluster formation. The equilibrium structure of the methyl group relative to the hydroxyl group therefore remains as in the monomer staggered. This assumption determines the orientation of the methyl group in the cluster. It has to be emphasized that the specification of the conformation of the methyl group has not been determined from our experiment, but from a comparison to the methanol monomer. Fig. 2 shows one of the four possible experimentally determined structure of the phenol–methanol cluster and the definitions of the structural parameters.

Table 1 presents the experimental rotational constants for the electronic ground state of the cluster, together with the results of ab initio calculation at different levels of theory.

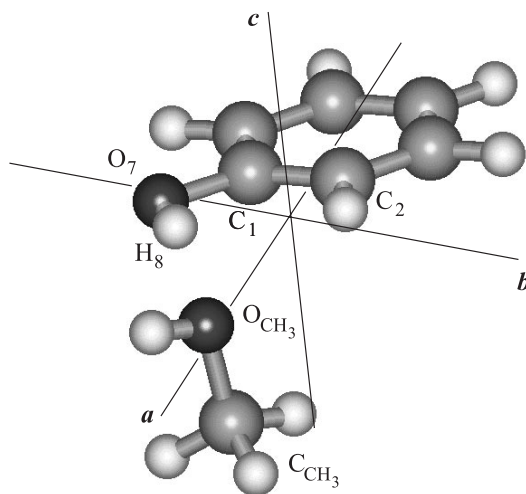


Fig. 2. Definition of the structural parameters of phenol–methanol, given in Tables 2 and 4 as described in the text.

Table 1  
Experimental and calculated rotational constants of phenol(CH<sub>3</sub>OH)<sub>1</sub> in the electronic ground state

|                | Experi-<br>ment <sup>a</sup> | 6-31G(d,p) |       |      |      |      | 6-311G(d,p) |      | 6-31++G(d,p) |      | aug-cc-pVDZ |                  |
|----------------|------------------------------|------------|-------|------|------|------|-------------|------|--------------|------|-------------|------------------|
|                |                              | HF         | B3LYP | SVWN | MP2  | MP4  | B3LYP       | MP2  | B3LYP        | MP2  | B3LYP       | MP2 <sup>b</sup> |
| <i>A</i> (MHz) | 3290.8                       | 3786       | 3717  | 3250 | 3220 | 3268 | 3701        | 3209 | 3795         | 3049 | 3864        | 3061             |
| <i>B</i> (MHz) | 792.19                       | 691        | 718   | 935  | 845  | 823  | 721         | 852  | 690          | 859  | 679         | 872              |
| <i>C</i> (MHz) | 685.62                       | 606        | 627   | 798  | 734  | 714  | 629         | 737  | 605          | 743  | 596         | 755              |

<sup>a</sup> Ref. [21].

<sup>b</sup> Only the convergence criterion for energy change ( $<10^{-8}$  hartree) was reached due to the flatness of the potential.

Obviously, the HF method overestimates the *A* rotational constant by 15%, while *B* and *C* are underestimated by 13% and 12%, respectively. This means that the calculated structure is extended too much along the inertial *a*-axis of the cluster. Indeed, the structure which is shown in Fig. 3a can be identified with a translinear geometry like in phenol–water, with one hydrogen atom replaced by the methyl group.

The rotational constants, obtained with MP2/6-31G(d,p), show a better agreement with the experimental values. The *A* constant is underestimated by 2%, while *B* and *C* are overestimated by 7%. The significant difference to the HF results is due to a considerable “folding” of the cluster (Fig. 3c). The hydrogen bond is no longer quasi-linear (described by the angle  $\angle(\text{H}_8\text{--O}_7\text{--O}_{\text{CH}_3})$  in Table 2), the O atom of methanol does not lie in the plane of the aromatic ring (described by the dihedral angle  $\angle(\text{O}_{\text{CH}_3}\text{--O}_7\text{--C}_1\text{--C}_2)$  in Table 2) and the angle between the hydrogen bond and the C–O axis of methanol ( $\angle(\text{O}_7\text{--O}_{\text{CH}_3}\text{--C}_{\text{CH}_3})$ ) becomes smaller. Increasing the basis set to the triple split 6-311G(d,p), and the inclusion of diffuse functions (6-31++G(d,p)) does not improve the results. Also the employment of an augmented Dunning basis set of double zeta quality did not lead to a considerable improvement of the results at first sight. Nevertheless it has to be considered, that the experimentally determined structure is vibrationally averaged over the zero-point vibrations, while the calculated structure represents the geometry at the potential minimum. Optimization of the geometry at MP4(SDQ)/6-311G(d,p) level leads to an *A* rotational constant, which is less than 1% smaller than the experimental value, and to *B* and *C* constants which are 4% larger. Also the experimentally determined intermolecular param-

eters given in Table 2 agree very well with the MP4(SDQ) optimized structure. Nevertheless this calculation suffers from the extremely small basis set, which had to be chosen for this large system due to the limited computational resources.

The gradient corrected hybrid functional B3LYP, which contains a portion of electron correlation does only slightly better than the HF calculation. Using the 6-31G(d,p) basis set, the *A* constant is too large by 13%, while both other rotational constants are too small by 9% compared to the experimental values. The resulting structure is shown in Fig. 3b.

The known trend of LSDA to overestimate the correlation energy and to underestimate the exchange energy results in a structure in which the rotational constants of the short axis are considerably exaggerated (15%). The SVWN functional as implementation of the LSDA tends to overemphasize the strengths of van der Waals bonds over hydrogen bonds, therefore leading to a cluster structure, in which the methyl group of the methanol moiety is strongly bent toward the aromatic ring (Fig. 3d).

The comparison of the geometric parameters of the four possible cluster structures with the corresponding theoretical values suggests structure I as most probable. For the geometric structure in the electronically excited state a calculation at the CIS/6-31G(d,p) level has been performed, that yielded rotational constants, which are very close to the experimental ones (the deviation for all three rotational constants is smaller than 1%, cf. Table 3). With regard to the ground state calculations at HF level, this fact can only be contributed to a favorable case of error compensation. Reliable results for the electronically excited states can only be expected using correlated methods for

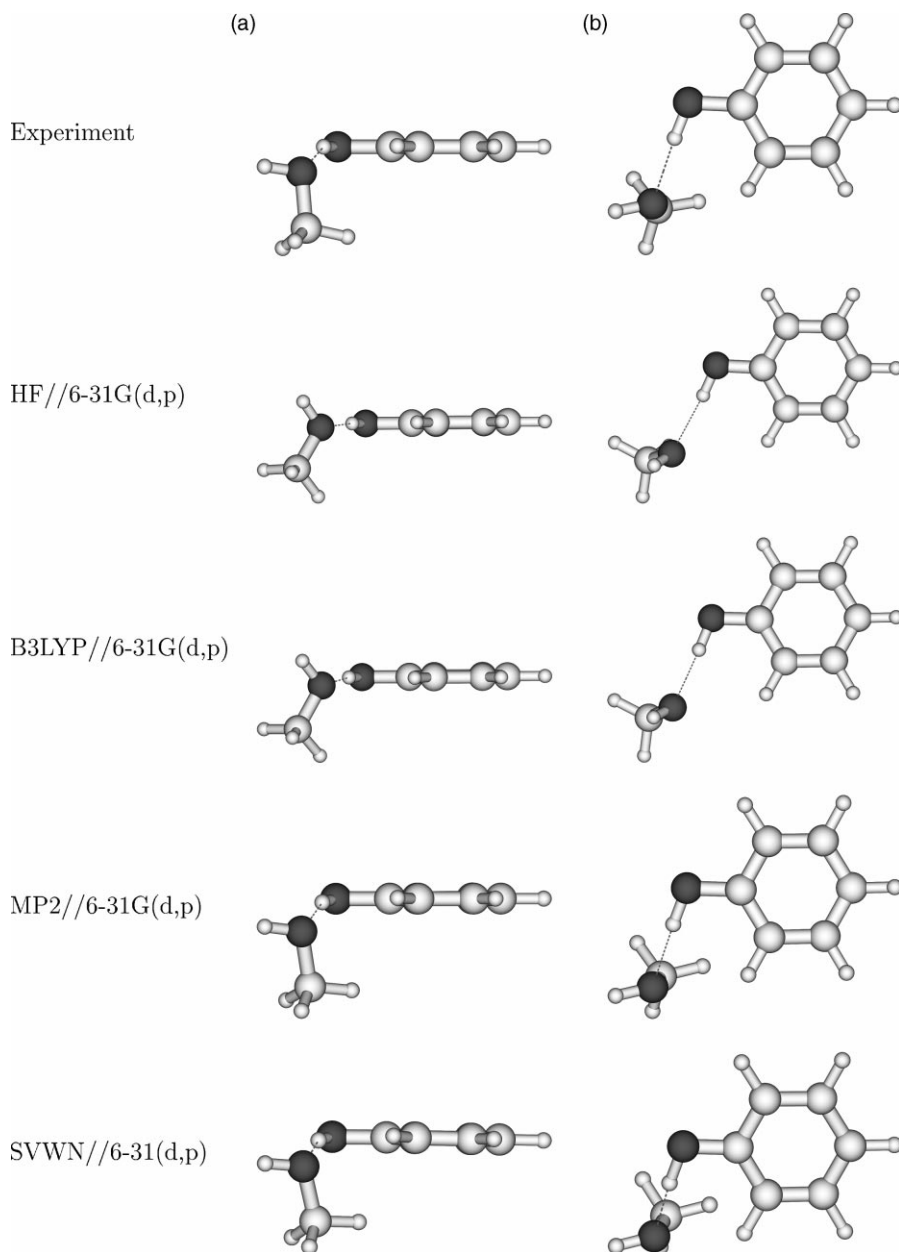


Fig. 3. (a) Top view of the calculated structures of phenol-methanol at the HF, B3LYP, MP2 and SVWN level of theory using the 6-31G(d,p) basis set, compared to the experimental structure and (b) side view of the calculated structures of phenol-methanol at the HF, B3LYP, MP2 and SVWN level of theory using the 6-31G(d,p) basis set, compared to the experimental structure.

the  $S_1$  state like CASPT2. In the present case of phenol-methanol, the required active space is too large to perform the calculations. Like in the electronic ground state the calculated  $S_1$ -geometry

is close to experimental structure I (Table 4). This seems to be a good clue towards this structure, because the transition intensities in the LIF spectrum exclude a change of sign of one  $\lambda_g$  upon

Table 2

Structural parameters of four possible structures of phenol(CH<sub>3</sub>OH)<sub>1</sub> in the S<sub>0</sub> state compared to structures calculated on the HF, B3LYP and MP2 level of theory with the 6-31G(d,p) basis set<sup>a</sup>

|   | Experiment     |                |                |                | Theory |        |       |       |
|---|----------------|----------------|----------------|----------------|--------|--------|-------|-------|
|   | 1 <sub>0</sub> | 2 <sub>0</sub> | 3 <sub>0</sub> | 4 <sub>0</sub> | HF     | B3LYP  | MP2   | MP4   |
| $d(\text{O}_7\text{-OCH}_3)$ (Å)                              | 2.824          | 3.006          | 3.027          | 3.199          | 2.891  | 2.784  | 2.775 | 2.809 |
| $\angle(\text{H}_8\text{-O}_7\text{-OCH}_3)$ (°)              | 13.74          | 13.98          | 14.28          | 13.70          | 3.5    | 4.97   | 12.10 | 11.32 |
| $\angle(\text{OCH}_3\text{-O}_7\text{-C}_1\text{-C}_2)$ (°)   | 14.52          | 14.47          | 14.17          | 14.26          | 2.5    | 4.86   | 18.09 | 15.98 |
| $\angle(\text{O}_7\text{-OCH}_3\text{-CCH}_3)$ (°)            | 105.73         | 89.89          | 88.16          | 74.17          | 116.1  | 108.87 | 93.94 | 95.82 |
| $\angle(\text{CCH}_3\text{-OCH}_3\text{-O}_7\text{-C}_1)$ (°) | 79.10          | 68.86          | 102.83         | 92.22          | 112.0  | 66.87  | 80.18 | 83.43 |

<sup>a</sup> Definitions of the distances, angles and dihedral angles and the numbering of the atoms are given in Fig. 2.

Table 3

Experimental rotational constants of phenol(CH<sub>3</sub>OH)<sub>1</sub> in the S<sub>1</sub> state and calculated with CIS/6-31G(d,p)

|                | Experiment | CIS  |
|----------------|------------|------|
| <i>A</i> (MHz) | 3310.5(1)  | 3299 |
| <i>B</i> (MHz) | 775.89(6)  | 779  |
| <i>C</i> (MHz) | 664.25(5)  | 671  |

electronic excitation, which would give rise to a change to one of the other three structures.

The MP2 calculations proved to reproduce the geometry of the cluster better than the DFT calculations with the B3LYP functional. On the other hand the vibrational frequencies, needed for the ZPE correction are better for B3LYP (see Section 3.2). Using both methods, the dissociation energy has been calculated. Table 5 presents the well depth  $D_e$  of the cluster relative to the monomers, which is corrected for BSSE using the counterpoise procedure of Boys and Bernardi [30], and the BSSE corrected binding energy  $D_0$  of phenol-methanol in the electronic ground state, together with the experimental value of Courty et al. [18].

Both B3LYP and MP2 show good agreement with the experimental value. The deviation of the B3LYP value (11%) from the experimental one is a little bit less than that of MP2, which can be traced back to the unreliable vibrational MP2 frequencies of the cluster (cf. Section 3.2).

### 3.2. Intermolecular vibrations

The experimental vibrational frequencies [17] for the electronic ground state and the calculated harmonic frequencies are given in Table 6. Their designation follows the nomenclature of Schütz et al. [5] for the phenol-water cluster. The three vibrations with lowest frequencies are of rotational parentage of the methanol moiety about its inertial axes, while the higher frequency vibrations can be described as descending from translational motions of the methanol moiety.

Regarding the large difference between the experimental structure and the HF optimized geometry, the correspondence between the experimental frequencies and the HF/6-31G(d,p) values has to be viewed as purely accidental. Especially

Table 4

Structural parameters of four possible structures of phenol(CH<sub>3</sub>OH)<sub>1</sub> in the S<sub>1</sub> state compared to the structure calculated on the CIS level of theory with the 6-31G(d,p) basis set<sup>a</sup>

|   | Experiment     |                |                |                | Theory |
|---|----------------|----------------|----------------|----------------|--------|
|   | 1 <sub>1</sub> | 2 <sub>1</sub> | 3 <sub>1</sub> | 4 <sub>1</sub> | CIS    |
| $d(\text{O}_7\text{-OCH}_3)$ (Å)                              | 2.701          | 2.999          | 3.056          | 3.327          | 2.831  |
| $\angle(\text{H}_8\text{-O}_7\text{-OCH}_3)$ (°)              | 13.79          | 15.50          | 12.05          | 11.69          | 7.66   |
| $\angle(\text{OCH}_3\text{-O}_7\text{-C}_1\text{-C}_2)$ (°)   | 12.79          | 12.56          | 12.15          | 12.36          | 13.25  |
| $\angle(\text{O}_7\text{-OCH}_3\text{-CCH}_3)$ (°)            | 116.25         | 89.27          | 84.63          | 62.56          | 110.09 |
| $\angle(\text{CCH}_3\text{-OCH}_3\text{-O}_7\text{-C}_1)$ (°) | 68.53          | 54.82          | 117.08         | 101.55         | 73.10  |

<sup>a</sup> Definitions of the distances, angles and dihedral angles and the numbering of the atoms is given in Fig. 2.

Table 5  
Experimental and calculated binding energies of phenol  
(CH<sub>3</sub>OH)<sub>1</sub> in the electronic ground state

|                                 | Experiment               | B3LYP | MP2   |
|---------------------------------|--------------------------|-------|-------|
| $D_e$ (kcal mol <sup>-1</sup> ) | –                        | 6.857 | 6.887 |
| $D_0$ (kcal mol <sup>-1</sup> ) | 6.11 ± 0.18 <sup>a</sup> | 5.475 | 5.206 |

Both B3LYP and MP2 values are corrected for BSSE. The ZPE has been calculated from the vibrational frequencies of the B3LYP/6-31G(d,p) and MP2/6-31G(d,p) optimized geometries.

<sup>a</sup> From Ref. [18].

for the  $\beta_2$ -vibration with a small reduced mass and small force constant (cf. Table 7) anharmonicity has to be considered [16]. Also the vibrational frequencies obtained with the B3LYP functional match the experimental values well. Especially with the aug-cc-VDZ basis a very good agreement of the frequencies of all intermolecular vibrations could be obtained.

The agreement between experimental and calculated frequencies at the MP2 level of theory is quite disappointing. All calculated frequencies are distinctly too high and especially the stretching vibration shows a large deviation from the experimental value. For comparable cluster systems, the stretching vibration has always found to be quite harmonic, and its frequency was predicted well at this level of theory. This difference has the same reason as the deviation of the calculated structure from the experimental one. The correlation interaction between methanol and phenol is overemphasized, thus leading to a larger force constant for the stretching vibration (see Table 7). All intermolecular normal modes, calculated at the MP2 level of theory show larger force constants compared to the HF and B3LYP calculations. This increase is only partially compensated for by the larger reduced masses, leading to distinctly higher vibrational frequencies. It should be emphasized, that all calculated vibrational frequencies in Table 6 are unscaled. The good correspondence of the harmonic HF/6-31G(d,p) intermolecular vibrational frequencies to the experimental values shows, that the prediction of the geometric structure of the cluster from an ab initio intermolecular potential energy surface is difficult and may lead to wrong results. The intermolecular vibrations in the electronically excited state, which have been cal-

Table 6  
Vibrational frequencies of the phenol-methanol cluster in the electronic ground state

| Experi-<br>ment <sup>a</sup><br>S <sub>0</sub> | Assign-<br>ment <sup>b</sup> | Harmonic frequencies |            |            |            |            |            |       |
|--|------------------------------|----------------------|------------|------------|------------|------------|------------|-------|
|  |                              | HF                   |            |            | B3LYP      |            |            |       |
|  |                              | 6-31G(d,p)           | 6-31G(d,p) | 6-31G(d,p) | 6-31G(d,p) | 6-31G(d,p) | 6-31G(d,p) |       |
| 22   | $\rho_2$                     | 17.3                 | 13.5       | 20.9       | 21.8       | 20.4       | 34.1       | 28.7  |
| 35   | $\tau$                       | 30.2                 | 31.4       | 36.3       | 34.4       | 31.9       | 61.6       | 54.3  |
| 55   | $\beta_2$                    | 54.6                 | 59.7       | 53.4       | 56.1       | 52.5       | 89.3       | 77.3  |
| 75   | $\rho_1$                     | 70.3                 | 77.3       | 80.9       | 79.0       | 76.0       | 101.5      | 94.3  |
| 91   | $\beta_1$                    | 90.4                 | 102.8      | 97.7       | 104.4      | 98.9       | 143.3      | 121.9 |
| 162  | $\sigma$                     | 158.1                | 188.2      | 188.2      | 173.2      | 165.0      | 198.2      | 186.8 |

<sup>a</sup> From Ref. [17].

<sup>b</sup> The assignment is based on Ref. [17], except for the  $\rho_1$  vibration which was assigned to the transition at 62 cm<sup>-1</sup>.



Table 7  
Vibrational frequencies, reduced masses and force constants for the respective motions of the phenol(CH<sub>3</sub>OH)<sub>1</sub> cluster in the S<sub>0</sub> state, calculated with the 6-31G(d,p) basis set

| Assignment | HF                            |                    |                                    | B3LYP                         |                    |                                    | MP2                           |                    |                                    |
|------------|-------------------------------|--------------------|------------------------------------|-------------------------------|--------------------|------------------------------------|-------------------------------|--------------------|------------------------------------|
|            | Frequency (cm <sup>-1</sup> ) | Reduced mass (amu) | Force constant (Nm <sup>-1</sup> ) | Frequency (cm <sup>-1</sup> ) | Reduced mass (amu) | Force constant (Nm <sup>-1</sup> ) | Frequency (cm <sup>-1</sup> ) | Reduced mass (amu) | Force constant (Nm <sup>-1</sup> ) |
| $\rho_2$   | 17.3                          | 3.1655             | 0.06                               | 13.5                          | 3.0825             | 0.03                               | 38.0                          | 3.7166             | 0.32                               |
| $\tau$     | 30.2                          | 3.1023             | 0.17                               | 31.4                          | 3.1735             | 0.18                               | 60.3                          | 3.0840             | 0.66                               |
| $\beta_2$  | 54.6                          | 1.3220             | 0.23                               | 59.7                          | 1.5509             | 0.33                               | 80.7                          | 1.9705             | 0.76                               |
| $\rho_1$   | 70.3                          | 4.6350             | 1.35                               | 77.3                          | 4.5533             | 1.60                               | 102.7                         | 2.7472             | 1.71                               |
| $\beta_1$  | 90.4                          | 2.2783             | 1.10                               | 102.8                         | 1.8125             | 1.13                               | 140.6                         | 1.7182             | 2.00                               |
| $\sigma$   | 158.1                         | 4.9843             | 7.34                               | 188.2                         | 5.0084             | 10.45                              | 199.1                         | 4.7240             | 11.03                              |

Table 8  
Vibrational frequencies of the phenol–methanol cluster in the electronically excited state

| Experiment <sup>a</sup> | Assignment <sup>b</sup> | Harmonic frequencies CIS <sup>c</sup> |
|-------------------------|-------------------------|---------------------------------------|
| S <sub>1</sub>          |                         |                                       |
| 27                      | $\rho_2$                | 38.8                                  |
| 31                      | $\tau$                  | 44.7                                  |
| 45                      | $\beta_2$               | 74.3                                  |
| 70                      | $\rho_1$                | 93.4                                  |
| 96                      | $\beta_1$               | 124.0                                 |
| 176                     | $\sigma$                | 177.6                                 |

<sup>a</sup> From Ref. [17].

<sup>b</sup> The assignment is based on Ref. [17].

<sup>c</sup> Using the 6-31G(d,p) basis set.

culated at the CIS/6-31G(d,p) level of theory are given in Table 8. Again the agreement between experimental and theoretical frequencies is good, but regarding the rather low level of theory has to be considered as accidental.

The rotational constants, which are obtained from the ab initio calculations represent the geometry of the cluster at the minimum of the potential energy surface, while the experimentally determined rotational constants reflect a geometry which is averaged over all zero point vibrational motions. The normal coordinates  $Q$  may be used to correct for this effect. A correction of the rotational constants has to consider the mean square displacements of  $Q^2$ , which are already contained in the harmonic approximation, the mean square displacement of  $Q$  due to anharmonic corrections, and the Coriolis interaction between nearly degenerate pairs of normal modes. The influence of the third point on the rotational constants is small in the asymmetric phenol–methanol cluster, while the second of these points demands the evaluation of the complete anharmonic force field.

### 3.3. Barrier to internal rotation

From the analysis of the perturbation of the rovibronic spectrum, the ratio  $V_3/F$  could be detected experimentally in the electronic ground and excited state to 32.16 and 27.65, respectively [21]. With these reduced barrier heights we simulated the pure torsional spectrum for phenol–methanol. The Hamiltonian for the internal rotation problem

Table 9  
Vibrational frequencies of the phenol–methanol cluster in the electronically excited state

| Assignment                        | Calculated | Experiment <sup>a</sup> |
|-----------------------------------|------------|-------------------------|
| 0a <sub>1</sub> ← 0a <sub>1</sub> | 0          | 0                       |
| 1e ← 1e                           | 0.14       | 0.12 <sup>b</sup>       |
| 2e ← 1e                           | 66.3       | (66) <sup>c</sup>       |
| 3a <sub>1</sub> ← 0a <sub>1</sub> | 73.5       | 74                      |
| 4e ← 1e                           | 128.4      | 128                     |
| 5e ← 1e                           | 172.8      | 167                     |

<sup>a</sup> From Ref. [17].

<sup>b</sup> Splitting from Ref. [21].

<sup>c</sup> This transition was not assigned but can be seen in Fig. 2 of Ref. [17].

was set up in the basis of free rotor wave functions and diagonalized in order to obtain the torsional levels for both electronic states. Table 9 compares the calculated torsional transitions with so far unassigned vibronic transitions from the LIF spectrum of Ref. [17]. The good agreement between observed and calculated torsional transitions confirms the correctness of the barrier determination in Ref. [21].

Under the assumption of a simple one-dimensional methyl rotation, the internal rotation constant  $F$  were 158.1 and 158.2 GHz in the  $S_0$  and  $S_1$  state, respectively. This would lead to torsional barriers of 170 cm<sup>-1</sup> in the electronic ground state and of 146 cm<sup>-1</sup> in the excited state which differ considerably from the  $V_3$ -barrier in the ground state of free methanol of 376.8 cm<sup>-1</sup> [31]. This reduction in barrier height upon cluster formation is known for many complexes of methanol. In the methanol dimer the barrier to internal rotation in the acceptor methanol was determined to be 120 cm<sup>-1</sup> [32] and in the aniline–methanol cluster to be 215 cm<sup>-1</sup> [33]. Fraser et al. [34] proposed that this decrease in barrier height is an artifact, due to the coupling of the internal rotation, to the librational motion of the methanol molecule about its inertial  $a$ -axis. The stronger the methanol molecule is bound, the larger is the hindrance potential for the librational motion and the closer is the value of  $F$  to the contribution from the moment of inertia of the methyl top (158 GHz).

We calculated the hindrance potential for free methanol (for comparison with the cluster) and for

phenol–methanol on the HF, B3LYP and MP2 level of theory, using the 6-31G(d,p) basis set. The torsional angle was defined as dihedral angle which is formed by the plane H<sub>1</sub>(methyl)–C–O with the plane C–O–H(hydroxyl), and was stepped in increments of 5°. All other internal coordinates, including those of the methyl group were allowed to relax for each torsional angle. The motion calculated hereby is not a simple one-dimensional rotation of the methyl group, but describes a minimum energy path along all internal coordinates, which connects neighboring minima. It therefore represents a lower limit for the calculated value of the torsional barrier (cf. Table 10). Fig. 4 shows the torsional potentials for methanol and the phenol–methanol cluster. For the monomer torsional barriers of 453 (HF/6-31G(d,p)), 473 cm<sup>-1</sup> (B3LYP/6-31G(d,p)) and 500 cm<sup>-1</sup> (MP2/6-31G(d,p)) had been obtained (uncorrected for ZPE vide supra), compared to the experimental value of 377 cm<sup>-1</sup>. Using larger basis sets and higher order perturbation theory a closer agreement to the value of a global fit to experimental values can be obtained, as has been shown by [27]. In order to calculate the relative change in barrier height upon complexation with phenol, we had to restrict ourselves to the level of theory described above.

The torsional barrier in the cluster, at MP2/6-31G(d,p) level of theory, calculated with the same strategy is 492 cm<sup>-1</sup>. This is almost the same barrier as calculated for free methanol at the same level of theory. Using B3LYP/6-31G(d,p), the torsional barrier is reduced to 365 cm<sup>-1</sup> upon complexation, while for HF/6-31G(d,p) only a

Table 10  
Torsional barriers for methanol and the phenol–methanol cluster obtained with different methods and levels of theory

| Method     | Torsional barrier (cm <sup>-1</sup> ) |                               |                        |
|------------|---------------------------------------|-------------------------------|------------------------|
|            | Methanol (relaxed PES)                | Phenol–methanol (relaxed PES) | Phenol–methanol (STQN) |
| HF         | 453                                   | 426                           | –                      |
| B3LYP      | 473                                   | 365                           | 366                    |
| MP2        | 500                                   | 493                           | 483                    |
| Experiment | 377.8 <sup>a</sup>                    | 170 <sup>b</sup>              | 170                    |

<sup>a</sup> From Ref. [31].

<sup>b</sup> Assuming a torsional constant  $F$  of 5.2 cm<sup>-1</sup>.

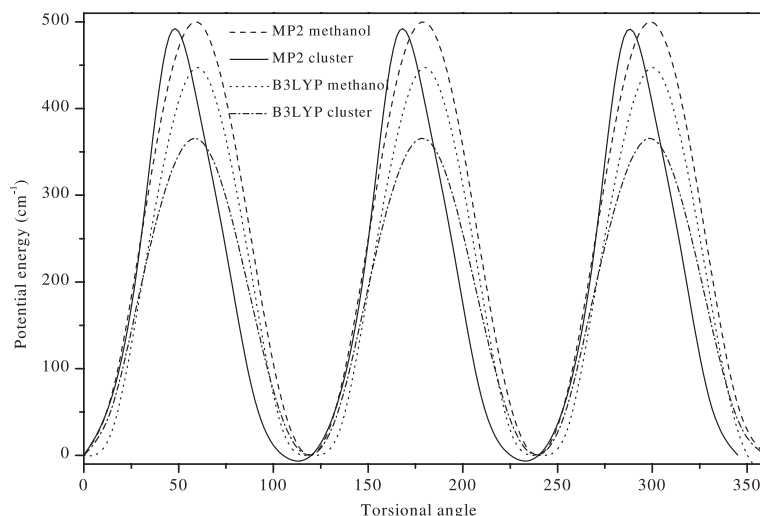


Fig. 4. Calculated barrier to internal rotation of the methyl group in methanol and the phenol–methanol cluster. The four traces show the variation of the MP2 and B3LYP energy of methanol with the torsional angle, and the corresponding MP2 and B3LYP energies of the cluster, calculated using the 6-31G(d,p) basis set.

slight reduction from 453 to 426  $\text{cm}^{-1}$  is obtained. Thus the calculated reductions of barrier heights upon cluster formation are 6% for HF, 19% for B3LYP and 2% for MP2, compared to a reduction of the experimental barrier of 55%. These results imply that the decrease of the value for the reduced barrier height  $V_3/F$  (from 32.16 to 27.65) upon complexation is rather due to a change of the internal rotation constants  $F$  than to the torsional barrier  $V_3$ .

The value obtained for the relaxed PES at MP2 level of theory was checked against a barrier, which had been calculated for the transition state, optimized using the STQN [28,29]. The transition state found, using this method, is 483  $\text{cm}^{-1}$  above the bottom of the potential, which is close to the value of the relaxed PES (vide supra). It is a little bit smaller than the barrier, obtained from the potential energy scan, what can be attributed to the relatively large step size in the optimization of the PES.

A comparison of the energies of the MP2 optimized structures with the HF energies at the corresponding MP2 optimized geometries shows the interesting result that the torsional barrier of the cluster is reduced from 426 to 340  $\text{cm}^{-1}$ . This shows again the large influence of electron cor-

relation for the intra-cluster forces, which determines the torsional barriers as well as the geometrical structure. Fig. 5 shows, that the relative difference between the HF and MP2 energies at the MP2 optimized structures is minimal for 0° and 120° and maximal for 45° and 90°.

The calculated MP2/6-31G(d,p) potential can be well approximated by a single  $V_3$  term of the following Fourier series:

$$E_t = \frac{1}{2} \sum_n V_n (1 - \cos n\alpha) \quad (1)$$

with  $V_3 = 483 \text{ cm}^{-1}$ . The minimum of the calculated MP2/6-31G(d,p) potential is shifted by 1.5° with respect to the minimum of the pure methanol at 120°. In order to check if this shift is not an artifact due to numerical inaccuracies in the calculation, the direction of rotation in the calculation was reversed and the step width was changed to 1°, yielding the same shift. This small potential shift can be explained by the additional dispersive interaction, which favors a slightly different equilibrium geometry. The variation of two molecular parameters, that is the angle of the CO axis with the aromatic plane, and the distance of the  $\text{C}_{\text{CH}_3}$  to the  $\text{C}_1$  of phenol, upon change of the torsional

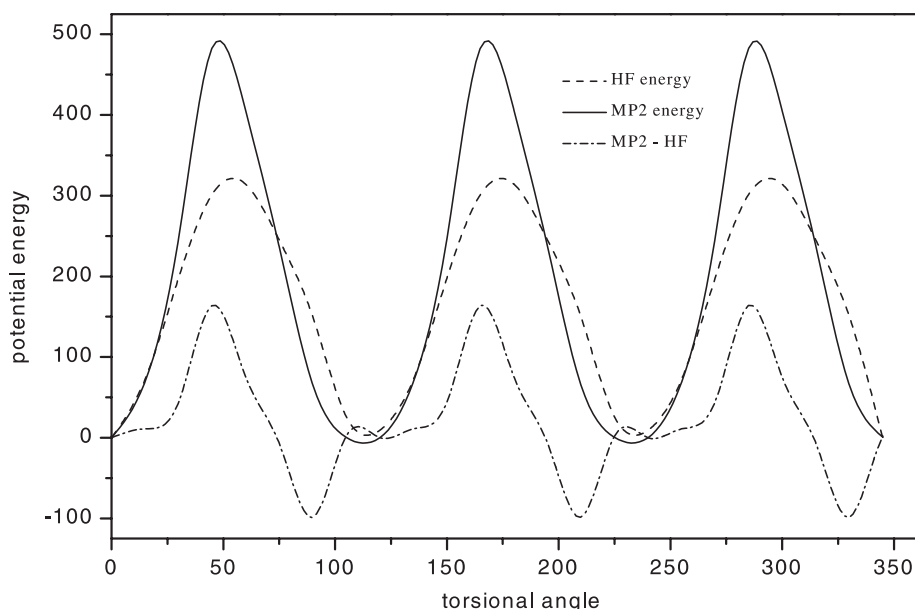


Fig. 5. Difference between the HF energy calculated at the optimized MP2 geometries and the respective MP2 energies.

angle have been evaluated. This angle and distance are minimal when one of the methyl H-atoms points towards the aromatic ring and are at maximum when they are in a staggered position. This is in agreement with the concept of a (binding) dispersive interaction between the methyl group and the  $\pi$ -system. Because the maxima and minima of interaction between the methyl group and the aromatic  $\pi$ -system do not coincide with the extrema of the potential barrier, there is a slight phase shift of the barrier due to the additional interaction in the cluster compared to the monomer.

The relaxation of all other coordinates of the cluster during the torsion changes especially the relative coordinates which determine the orientation of the monomer units. There is a considerable amount of coupling with the  $\rho_2$  and the  $\beta_2$  vibrational modes. The first represents a librational motion with the inertial  $a$ -axis of methanol as axis of rotation, while the second one can be described as a bending mode of the methanol moiety. Thus the 'real' motion is not just the torsion of the methyl group, but a rather complex motion, which considerably couples with at least two normal modes of the cluster. The value of the internal

rotor constant  $F$  is not conserved along this path, i.e.  $F$  is a function of the torsional angle and probably larger than expected for a pure torsional motion of the methyl group.

#### 4. Conclusions

The geometry of the hydrogen bonded phenol–methanol cluster which has been determined experimentally by high resolution LIF spectroscopy could be reproduced well at the MP2/6-31G(d,p) level of theory. The orientation of the methanol moiety with respect to the phenyl ring is strongly dependent on the balance between hydrogen bond and the interaction between the aromatic  $\pi$ -system and the methyl group. In order to describe them properly, electron correlation has to be taken into account. This can clearly be seen by the failure of the Hartree–Fock method as well as density functional methods, which contain only partially HF exchange in describing the structure.

The dissociation energy  $D_0$  of the cluster, calculated with MP2 and B3LYP using the rather small 6-31G(d,p) basis, shows good agreement with the experimental one [18].

The computation of the intermolecular vibrations is delicately dependent on the method and basis set employed and seems in this case not to be very reliable for a determination of the cluster structure.

The calculation of the torsional barrier of the methyl group in the methanol moiety shows no evident decrease in barrier height of the phenol–methanol cluster compared to the methanol monomer. Thus we conclude, that the experimental finding of a considerable decreasing value of  $V/F$  upon complexation in phenol–methanol is mostly due to an increasing value of the internal rotor constant  $F$ . The phase of the barrier is slightly altered by the interaction of the methyl group with the aromatic ring.

## Acknowledgements

We would like to thank especially Professor Kleinermanns for his steady interest in this work and for many helpful discussions. We also thank Dr. Georg Jansen for helpful comments and discussions. The financial support of the Deutsche Forschungsgemeinschaft (SCHM 1043/7-1) is gratefully acknowledged.

## References

- [1] H. Abe, N. Mikami, M. Ito, *J. Phys. Chem.* 86 (1982) 1768.
- [2] A. Sur, P.M. Johnson, *J. Chem. Phys.* 84 (1986) 1206.
- [3] R.J. Stanley, A.W. Castleman Jr., *J. Chem. Phys.* 94 (1991) 7744.
- [4] R.J. Lipert, S.D. Colson, *J. Chem. Phys.* 89 (1988) 4579.
- [5] M. Schütz, T. Bürgi, S. Leutwyler, T. Fischer, *J. Chem. Phys.* 98 (1993) 3763.
- [6] G. Berden, W.L. Meerts, M. Schmitt, K. Kleinermanns, *J. Chem. Phys.* 104 (1996) 972.
- [7] M. Gerhards, M. Schmitt, K. Kleinermanns, W. Stahl, *J. Chem. Phys.* 104 (1996) 967.
- [8] M. Schmitt, C. Jacoby, K. Kleinermanns, *J. Chem. Phys.* 108 (1998) 4486.
- [9] R.M. Helm, H.-P. Vogel, H.J. Neusser, *J. Chem. Phys.* 108 (1998) 4496.
- [10] T. Ebata, M. Furukawa, T. Suzuki, M. Ito, *J. Opt. Soc. Am. B* 7 (1990) 1890.
- [11] O. Dopfer, K. Müller-Dethlefs, *J. Chem. Phys.* 101 (1994) 8508.
- [12] T. Watanabe, T. Ebata, S. Tanabe, N. Mikami, *J. Chem. Phys.* 105 (1996) 408.
- [13] S. Tanabe, T. Ebata, M. Fujii, N. Mikami, *Chem. Phys. Lett.* 215 (1993) 347.
- [14] H. Abe, N. Mikami, M. Ito, Y. Udagawa, *J. Phys. Chem.* 86 (1982) 2567.
- [15] T.G. Wright, E. Cordes, O. Dopfer, K. Müller-Dethlefs, *J. Chem. Soc. Faraday Trans.* 89 (1993) 1601.
- [16] M. Gerhards, K. Beckmann, K. Kleinermanns, *Z. Physik D* 29 (1994) 223.
- [17] M. Schmitt, H. Müller, U. Henrichs, M. Gerhards, W. Perl, C. Deussen, K. Kleinermanns, *J. Chem. Phys.* 103 (1995) 584.
- [18] A. Courty, M. Mons, B. Dimicoli, F. Piuze, V. Brenner, P. Millié, *J. Phys. Chem. A* 102 (1998) 4890.
- [19] R.M. Helm, H.J. Neusser, *Chem. Phys.* 239 (1998) 33.
- [20] U. Gudladt, Mikrowellenspektroskopische Untersuchungen des Komplexes Phenol–Methanol, MS thesis, Christian Albrechts Universität, Kiel, 1996.
- [21] M. Schmitt, J. Küpper, D. Spangenberg, A. Westphal, *Chem. Phys.* 254 (2000) 349.
- [22] M.J. Frisch, G.W. Trucks, H.B. Schlegel, G.E. Scuseria, M.A. Robb, J.R. Cheeseman, V.G. Zakrzewski, J.A. Montgomery Jr., R.E. Stratmann, J.C. Burant, S. Dapprich, J.M. Millam, A.D. Daniels, K.N. Kudin, M.C. Strain, O. Farkas, J. Tomasi, V. Barone, M. Cossi, R. Cammi, B. Mennucci, C. Pomelli, C. Adamo, S. Clifford, J. Ochterski, G.A. Petersson, P.Y. Ayala, Q. Cui, K. Morokuma, D.K. Malick, A.D. Rabuck, K. Raghavachari, J.B. Foresman, J. Cioslowski, J.V. Ortiz, A.G. Baboul, B.B. Stefanov, G. Liu, A. Liashenko, P. Piskorz, I. Komaromi, R. Gomperts, R.L. Martin, D.J. Fox, T. Keith, M.A. Al-Laham, C.Y. Peng, A. Nanayakkara, C. Gonzalez, M. Challacombe, P.M.W. Gill, B. Johnson, W. Chen, M.W. Wong, J.L. Andres, C. Gonzalez, M. Head-Gordon, E.S. Replogle, J.A. Pople, *GAUSSIAN 98*, Revision A.7, Gaussian, Inc., Pittsburgh, PA, 1998.
- [23] J.C. Slater, *Quantum Theory of Molecular and Solids, The Self-Consistent Field for Molecular and Solids*, vol. 4, McGraw-Hill, New York, 1974.
- [24] S.J. Vosko, L. Wilk, M. Nusair, *Can. J. Phys.* 58 (1980) 1200.
- [25] A.D. Becke, *Phys. Rev. A* 38 (1988) 3098.
- [26] C. Lee, W. Yang, R. Parr, *Phys. Rev. B* 37 (1988) 785.
- [27] L.-H. Xu, R.M. Lees, J. Hougen, *J. Chem. Phys.* 110 (1999) 3835.
- [28] C. Peng, P.Y. Ayala, H.B. Schlegel, M.J. Frisch, *J. Comp. Chem.* 17 (1996) 49.
- [29] C. Peng, H.B. Schlegel, *Israel J. Chem.* 33 (1994) 449.
- [30] S.F. Boys, F. Bernardi, *Mol. Phys.* 19 (1970) 553.
- [31] M.C.L. Gerry, R.M. Lees, G. Winnewisser, *J. Mol. Spectrosc.* 61 (1976) 231.
- [32] F.J. Lovas, S.P. Belov, M.Y. Tretyakov, W. Stahl, R.D. Suenram, *J. Mol. Spectrosc.* 170 (1995) 478.
- [33] M. Haeckel, W. Stahl, *J. Mol. Spectrosc.* 198 (1999) 263.
- [34] G.T. Fraser, F.J. Lovas, R.D. Suenram, *J. Mol. Spectrosc.* 167 (1994) 231.